International Journal of Trendy Research in Engineering and Technology
Volume 10 Issue 3 June 2026
ISSN No. 2582-0958

OPTIMIZATION OF MIG WELDING PARAMETERS FOR ENHANCING THE HARDNESS OF MEDIUM CARBON STEEL USING RESPONSE SURFACE METHODOLOGY (RSM)

Shewangizaw Abu Abate
Industrial Development Researcher
Manufacturing Workshop, Foundry, Welding, and Maintenance Research Department
Manufacturing Industry Development Institute, Addis Ababa, Ethiopia
shewangizawabu99@gmail.com

Received 22 June 2026 Received in revised form 03 July 2026 Accepted 05 July 2026
Available Online 07 July 2026

ABSTRACT

Metal Inert Gas (MIG) welding parameters significantly affect weld quality, productivity, and manufacturing cost. This study aimed to optimize MIG welding parameters to improve weld hardness in medium carbon steel. A Design of Experiments (DOE) based on an Orthogonal Array (OA) was conducted on 22 samples. Response Surface Methodology (RSM) and Analysis of Variance (ANOVA) were used to evaluate the effects of welding current, voltage, travel speed, and gas flow rate. The optimal parameters were identified as 192 A current, 35 V voltage, 17.52 mm/s travel speed, and 14.54 L/min gas flow rate. Under these conditions, the predicted weld hardness reached 178.29 HV, representing a 4.88% improvement over the base material hardness of 170 HV. Validation through hardness testing confirmed the model's accuracy. The results demonstrate that RSM is an effective tool for enhancing weld quality and improving the structural performance of welded components in manufacturing applications.

Keywords: MIG Welding, Process Optimization, Response Surface Methodology (RSM), ANOVA, Medium Carbon Steel, Hardness Testing.

1. INTRODUCTION

Welding is one of the most important manufacturing processes used to permanently join similar or dissimilar materials. The quality of a welded joint depends on several process parameters, including welding current, voltage, travel speed, wire feed rate, electrode extension, torch angle, and shielding gas flow rate. Proper selection of these parameters is essential to achieve high-quality welds with desirable mechanical properties and surface finish[1-3]. Traditionally, welding parameters are selected through trial and error and operator experience. This approach is time-consuming, costly, and often fails to identify the optimal parameter combination. To overcome these limitations, statistical optimization techniques such as Design of Experiments (DOE), Analysis of Variance (ANOVA), and Response Surface Methodology (RSM) are widely used to establish relationships between welding input parameters and weld quality characteristics. These techniques help reduce experimental effort while improving process performance and product quality [4-6]. Metal Inert Gas (MIG) welding, also known as Gas Metal Arc Welding (GMAW), is one of the most widely used welding processes in manufacturing industries. It uses a continuously fed consumable electrode and shielding gas to produce strong and reliable joints. MIG welding is preferred because of its high productivity, ease of operation, low cost, portability, and suitability for a wide range of applications[3].

Among the mechanical properties of welded joints, hardness is an important indicator of weld quality and structural performance. During welding, the rapid heating and cooling cycles affect the microstructures of the weld metal and the heat-affected zone (HAZ), resulting in variations in hardness. Therefore, controlling welding parameters is essential for achieving the desired hardness and overall weld integrity [7,8]. This study focuses on optimizing MIG welding parameters to improve weld hardness in medium carbon steel. Statistical techniques, including DOE, ANOVA, and RSM, are employed to develop predictive models and determine the optimal combination of welding current, voltage, travel speed, and gas flow rate. The findings provide practical for improving weld practical guidance for improving weld quality and enhancing manufacturing efficiency [9].

2. MATERIAL AND METHODS

2.1Material Selection

The base material used in this study was AISI 1035 medium-carbon steel, with 0.394% carbon, selected for its high strength, impact resistance, and widespread use in automotive and machinery components. Test specimens were machined into plates measuring 100 mm × 100 mm × 6 mm with a 45-degree groove angle to prepare for two-pass rectangular butt welding.

The chemical composition of the base metal was verified via optical emission spectrometry at Akaki Basic Metal Industry (ABMI). Before welding, specimen surfaces were thoroughly cleaned to remove moisture, oil, grease, and oxides, minimizing porosity and ensuring proper weld pool fusion [10].The chemical composition of the steel used in this research is presented in Table 1

Table 1 Chemical composition of welding sample; source (spectrometer ABMI)

Element	Content (%)	Element	Content (%)	Element	Content (%)
C	0.394	Ni	<0.008	W	,0.040
Si	0.200	Al	0.040	Pb	<0.010
Mn	0.670	Co	<0.009	Sn	0.026
P	0.068	Cu	0.038	As	0.061
S	0.050	Nb	<0.005	Zr	0.003
Cr	0.018	Ti	0.001	B	0.009
Mo	<0.003	V	<0.002	Fe	98.4

2.2 Experimental Setup and Equipment

Welding was performed using a semi-automatic MIG353S welding machine. An AWS ER70S-6 solid wire electrode with a diameter of 1.2 mm was used as the consumable filler metal. Shielding was provided by 100% carbon dioxide (CO2) gas. To guarantee experimental consistency and isolate the effects of the control variables, external noise factors, including operator skill (same operator used throughout), ambient temperature, mechanical vibrations, squeeze time, and hold time, were held constant [11,12].

2.3 Design of Experiments (DOE) and Response Surface Methodology (RSM)

Response Surface Methodology (RSM) was employed to model and optimize the process parameters. Based on a screening phase, literature recommendations, and AWS standards, four critical control factors were varied across two operational levels [13].

Table 2. Process Parameters and Their Values at Different Levels

Symbol	Parameter name	Units	Level	
			Low	High
A	Current	Ampere	100	350
B	Voltage	Voltage	20	30
C	Travel speed	mm/min	15	20
D	Gas flow rate	Lit/mm	12	15

The experiment used an L22 Central Composite Design (CCD) matrix generated in Minitab 18, comprising 22 experimental runs (including 6 center points). This orthogonal array provides 21 total degrees of freedom (DOF), successfully satisfying the minimum required DOF to evaluate linear, quadratic, and two-factor interactive effects [14].

2.3.1 Design matrices

The design matrix chosen for the experiment was a central composite design consisting of a full factorial 31-run and half factorial 22-run coded conditions. The design matrix is constituted of a full replication of a 24 (32) factorial design, 16 cube points (one variable at its highest level +2 or lowest level -2 with all the other variables at the intermediate level 0), and 6 center points (all variables at the intermediate level 0). These experiments allowed the estimation of linear, quadratic, and linear-linear interactive effects of the welding parameters on the bead geometry[15,16].

2.3.2 Response surface methodology orthogonal array Design

To determine the effect on the response, we can use control factors during experimentation. Factors can be categorized based on a continuous variable, but only four controlled values are used in the experiment. According to the standard design of experiment, RSM OA design is L22, which shows the RSM orthogonal array selected the parameters and levels, four and two, respectively; the orthogonal array was selected from the array selector of RSM design of experiment in MINITAB 18 software package. Table.2 shows the standard orthogonal array for the design of the experiment.$\mathbf{2^n}$+2n+2(n-1)+1 full Central Composite design (CCD) [15]. From this table, the standard RSM full factorial design and 6 center point numbers of runs are 22.

Table 3 Standard RSM OA table, source (George E.P. Box and K. B. Wilson)

Design model	Run point	Number of factors			
		K=2	K=3	K=4	K=5
2^kCCD/BBD	Factorial point 2^k	4	8	16	32
	Axial point 2^k	4	6	8	10
	Center point	5	5	6	6
	Total	13	19	30	48
3^kdesign		9	27	81	243
Choice of α	Spherical design	1.4	1.73	2	2.24
	Rotatable design	1.4	1.68	2	2.38

parameters and their levels are given in Table 3. Each parameter has 1 degree of freedom (DOF =Number of levels-1), which 2-1=1, has a degree of freedom of 1, and the total DOF required for four parameters each of two levels. As per RSM's method, the total DOF of selected OA must be greater than or equal to the total DOF required for the experiment. So a standard L22 2-level OA having 7 DOF, mathematically 22-1=21, which is calculated as different between the total number of DOF (21) and one DOF for experiment, was selected for this analysis. In RSM, the word optimization implies the determination of the best levels of control factors for the best levels of control factors that maximize the RSM has 22 runs as desired output characteristics. The experiments that are conducted to determine the best combination for welding parameters are based on OA and are balanced with respect to all control factors. This, in turn, implies that the resource material and time required for the minimum experiments, source (MINITAB 18 software design package)

Table 4 Coded Parameters used for RSM, Source: (MINITAB 18)

Run order	Pt type	blocks	Control parameters			
			Current	Voltage	Travel speed	Gas flow rate
1	-1	2	225	35	17.5	13.5
2	-1	2	225	35	17.5	13.5
3	0	2	100	30	15	12
4	0	2	100	30	15	15
5	1	1	100	30	20	12
6	1	1	225	35	17.5	13.5
7	1	1	100	30	20	15
8	1	1	100	40	15	12
9	1	1	225	35	17.5	13.5
10	1	1	100	30	15	15
11	1	1	225	35	17.5	13.5
12	0	1	100	40	20	12
13	1	1	100	40	20	15
14	0	1	350	30	15	12
15	1	1	225	35	17.5	13.5
16	1	1	350	30	15	15
17	1	1	350	30	20	12
18	1	1	350	30	20	15
19	1	1	350	40	15	12
20	0	1	350	40	15	15
21	1	1	350	40	20	12
22	1	1	350	40	20	12

2.3.3 Design for experimental setup and specimen

In this experiment, the butt-weld joint of two similar AISI 1035Medium carbon steel plates of dimensions 100 x 100 x 6mm with a welding groove of 45° is used specimen was prepared using the specified material in dimensions to fabricate MIG welding of square butt joints. Welding experiments have been carried out using the MIG Welding process and an. In the welding experiment, standard wire AISI/AW ER70s-6 filler wire electrode with 1.2mm diameter has been used as a consumable electrode. Figure 1 shows a square butt joint and a geometry welding specimen for existing welding settings.

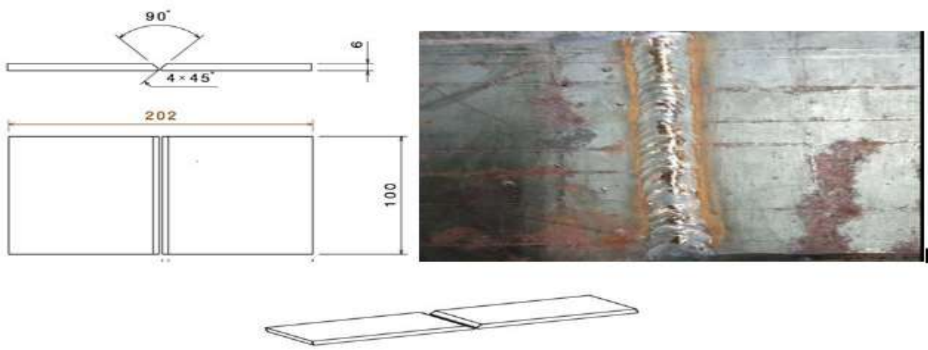

Figure 1 Photos of specimens during the welding experiment and Design of the welded workpiece in CATIA

Hardness testing of this specimen was performed in accordance with ASTM A370-14 standard using a Vickers hardness testing machine.

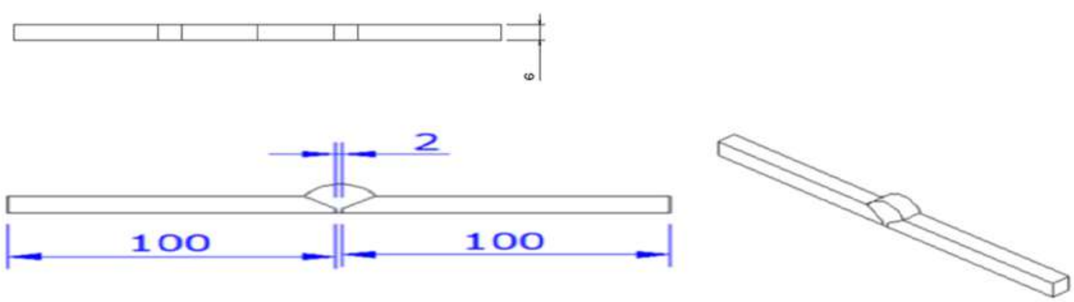

Figure 2 Welding specimen drawing for the hardness test

2.4 Quality Evaluation and Testing Protocols

2.4.1 Non-Destructive Testing (NDT)

To monitor surface and sub-surface integrity immediately following each welding trial, visual inspections were paired with Non-Destructive Testing (NDT). Liquid Penetrant Testing (LPT) and Magnetic Particle Inspection (MPI) were used to detect superficial flaws such as macro-cracks, spatter, surface porosity, and incomplete fusion boundaries [16].

2.4.2 Hardness Testing (Destructive Testing)

Vickers hardness testing was conducted in compliance with ASTM A370-14. Specimens were cross-sectioned and ground flush to ensure a flat, perpendicular surface profile. Testing was executed using a square-based diamond pyramid indenter under a 100 kgf load with a dwell time of 10–15 seconds. Hardness profiles (HV) were mapped continuously across three regions: the weld bead, the heat-affected zone (HAZ), and the parent metal. To improve mechanical performance, a "larger-the-better" signal-to-noise ratio characteristic was established for the hardness response[2], [17].

2.4.3 Metallographic and Microstructure Examination

Microstructural specimens (20 mm×20 mm×6 mm) were sectioned from the weldments in accordance with ASTM E23. Samples underwent progressive grinding, mirror-finish polishing, and chemical etching. Microstructural transitions across the weld bead, HAZ, and parent metal were characterized using an optical microscope equipped with a digital imaging system [2], [10].

3. DATA COLLECTION AND ANALYSIS

3.1 Liquid Penetrant Testing (LPT)

Eddy current, liquid penetrant, ultrasonic test, visual examinations, radiography testing, gamma-ray, x-ray, magnetic testing, and stethoscope test are categorized under NDT. Among these methods of tests, this research work has been done using LPT and MT because of their quality for detecting the amount of crack and porosity on the surface of the welded specimens, which depends on the thickness. The ultrasonic test was limited by thickness as well as availability. PT test for the data of porosity and other enhancements was shown on the product.

In this figure 3, welding defects are checked in different kinds of porosities for all samples for existed setting of the design of experiment using LP test, Source: Metal Industry Development Institute (MIDI).

Figure 3: Welded specimens after LPT modified setting, source: (Metal Industry Development Institute)

Table 5: Enhancements identified in MIG Welding of sixteen DOE samples

Sample	Crack	Undercut	Porosity	Penetration
Experiment	3, 7, 16, 19	4, 10, 17	1,5,8,9,13,14,20 21	2,6,11,12,15,18, 22

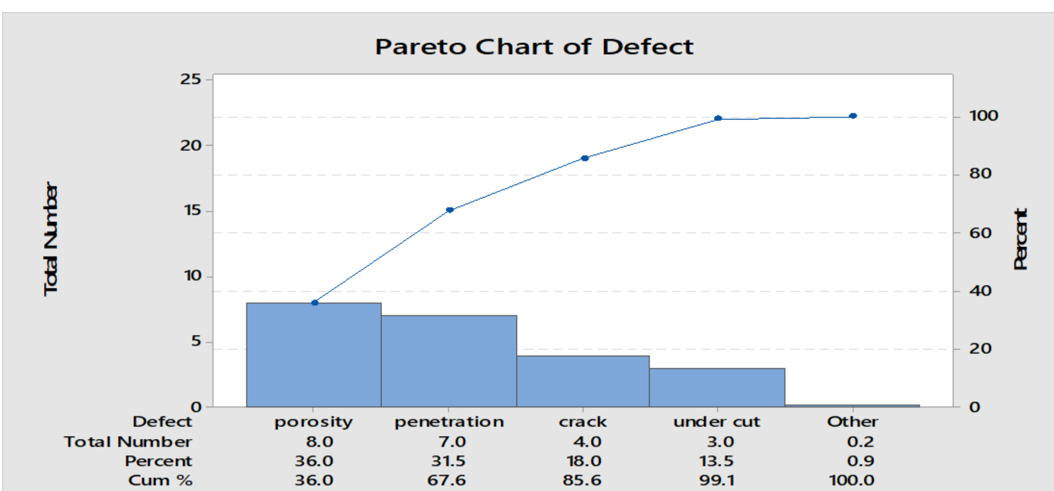

Figure 4 Pareto chart of defect type

The Pareto chart Consequently, addressing cracking or undercutting first yields negligible overall. To efficiently stabilize the MIG welding process and maximize performance, optimization efforts must focus strictly on resolving the root causes of these two dominant enhances by tuning parameters such as shielding gas flow rate, nozzle distance, welding current, voltage, and travel speed

3.2 Magnetic test (MT) for Optimization of the Samples

Magnetic testing (MT) is used to locate surface and slight subsurface discontinuities or defects in ferromagnetic materials. Such flaws present in the magnetized part will cause a magnetic field, i.e., flux, to leave the part.

While several different methods of magnetic particle test can be used, they all rely on this same general principle. Therefore, any magnetic particle test will be conducted by creating a magnetic field in a part and applying the magnetic particles to the test surface [18].

Figure 5 shows the MT result sheet, which is approved by the experts in the Metals Industry Development Institute (MIDI) for the MIG-welded plate metal weld bead in the quality assurance department.

Figure 5 Welding specimen's quality inspection sheet after (MT), Source: (MIDI)

3.3 Hardness testing.

The tests were conducted on carefully ground and polished samples using a minor and major load of 10 and 100 kg, respectively, and a 6mm diameter indenter ball. Each hardness test was performed three times, and the average was determined.

Table 6 Response Data for Design Matrix using 22 Runs Source: (MINITAB software design package) shows that the values of response for hardness test C35 (medium carbon steel) are to be analyzed in the MIDI lab quality department.

Figure 6 Vickers's hardness testing machine and hardness test specimen

Table 6 Response Data for Design Matrix using 22 Runs Source: (MINITAB software design package

Control Parameter Hardness test (N/mm2)

No	Current(A)	Voltage(v)	Travel speed	Gas flow rate(GFR)	HV(N/mm2)
1	225	35	17.5	13.5	188
2	225	35	17.5	13.5	180
3	100	30	15	12	174
4	100	30	15	15	167
5	100	30	20	12	172
6	225	35	17.5	13.5	168
7	100	30	20	15	182
8	100	40	15	12	165
9	225	35	17.5	13.5	160
10	100	40	15	15	174
11	225	35	17.5	13.5	152
12	100	40	20	12	164
13	100	40	20	15	178
14	350	30	15	12	188
15	225	35	17.5	13.5	183
16	350	30	15	15	167
17	350	30	20	12	161
18	350	30	20	15	158
19	350	40	15	12	152
20	350	40	15	15	178
21	350	40	20	12	174
22	350	40	20	12	182

For this study, three significant digits are implemented to reduce the amount of error occurring in numerical analysis. Amount of confidence interval 5% (0.05) and confidence level 95% (0.95) in this DOE for the CCD of RSM. If the probability (P) value is less than the confidence interval 0.05, it is significant; if the amount of P-value is greater than 0.05, it is insignificant. Our objective is to predict the maximum hardness test. For all DOE, larger-the-better characteristics are used.

3.4 Estimation of Regression Analysis using Mathematical Model

For this research work, second-order regression analysis of mathematical and analytical formulas for the response, in the case of the hardness test (HV), for the welding specimens of the 22 samples. Using regression constants $\mathbf{A_0}$, $\mathbf{A_1}$, $\mathbf{A_2}$, $\mathbf{A_3}$, $\mathbf{A_4}$, $\mathbf{A_{11}}$, $\mathbf{A_{22}}$, $\mathbf{A_{33}}$, $\mathbf{A_{44}}$, $\mathbf{A_{12}}$, $\mathbf{A_{13}}$, $\mathbf{A_{14}}$, $\mathbf{A_{23}}$, $\mathbf{A_{24}}$ and $\mathbf{A_{34}}$, are coefficient of (constant, current, travel speed, gas flow rate, current × current, travel speed × travel speed, gas flow rate × gas flow rate, current × voltage, current × travel speed, current × gas flow rate, error) regression analysis for parameter is $\mathbf{X_1}$=welding current,$\mathbf{X_2}$=arc voltage, $\mathbf{X_3}$=travel speed and$\mathbf{X_4}$=gas flow rate respectively. According to the maximum is the better concept of, no = 22 runs MIG welding to determine ANOVA for the hardness test. Factor (A) for the interaction effect of the Response for two-level factors.

Table 7 Analysis of Variance (ANOVA) for HV (Mpa)

Source	DF	Adj SS	Adj MS	F-Value	P-Value	Significant or non-significant
Model	11	10316.4	937.85	5.19	0.007	
Linear	4	3486.9	871.72	4.82	**0.020**	
A	1	1566.7	1566.67	8.66	**0.015**	**Significant**

B	1	113.3	113.34	0.63	0.447	non-significant
C	1	145.7	145.67	0.81	0.391	non-significant
D	1	935.7	935.67	5.17	**0.046**	**Significant**
Square	1	645.7	645.69	3.57	0.088	non-significant
A*A	1	645.7	645.69	3.57	0.088	non-significant
2-Way Interaction	6	4640.2	773.36	4.28	**0.021**	**Significant**
A*B	1	908.8	908.84	5.03	**0.049**	**Significant**
A*C	1	1085.1	1085.07	6	**0.034**	**Significant**
A*D	1	2.1	2.06	0.01	0.917	non-significant
B*C	1	69.3	69.34	0.38	0.55	non-significant
B*D	1	2171.7	2171.66	12.01	**0.006**	**Significant**
C*D	1	46.2	46.22	0.26	0.624	non-significant
Error	10	1808.2	180.82			
Lack-of-Fit	4	264.9	66.22	0.26	0.895	non-significant
Pure Error	6	1543.3	257.22			
Total	21	12124.6				
$S=13.4469	R-sq=85.09%	R-sq(adj) =68.68%		R-sq(pred)=51.09%		

The ANOVA results (Table 7) demonstrate that the fitted regression model is highly statistically significant (P = 0.007) with an R^2 of 85.09%, indicating the model explains most of the variability in the hardness data. Crucially, the Lack-of-Fit is non-significant (P = 0.895), confirming that the model accurately captures the true process topography without omitting critical higher-order terms.

Table 8: Estimated Regression Coefficients for HV (MPa)

Source	DF	Seq SS	Adj SS	Adj MS	F	P-value
Regression	11	10316.4	10316.4	937.85	5.09	**0.007**
Linear	4	4792.3	3486.9	871.72	4.82	**0.020**
Square	1	883.9	645.7	645.69	3.57	0.088
Interaction	6	4640.2	4640.2	773.36	4.28	**0.021**
Residual Error	10	1808.2	1808.2	180.82		
Lack-of-Fit	4	264.9	264.9	66.22	0.26	0.895
Pure Error	6	1543.3	1543.3	257.22		
Total	21	12124.6				

Table 8 the comparison of the Sequential Sum of Squares (Seq SS) and the Adjusted Sum of Squares (Adj SS) reveals a robust and statistically significant regression model (P = 0.007). In the linear block, the variance difference between Seq SS (4792.3) and Adj SS (3486.9) indicates minor multicollinearity or non-orthogonality among the primary factors. Conversely, the exact alignment of Seq SS and Adj SS values in both the quadratic (883.9) and interaction (4640.2) blocks mathematically illustrates that the two-way interactions (P = 0.021) and curvature effects have independent, non-overlapping predictive significance.

Regression Equation in coded Units

HV=1125 + 0.342 A - 29.41 B - 7.9 C - 62.0 D - 0.000790 A*A + 0.01271 A*B - 0.0278 A*C - 0.0021 A*D + 0.176 B*C + 1.698 B*D + 0.495 C*D.................................. (1)

$HV = 1125 + 0.342X_1 - 29.41X_2 - 7.9X_3 - 62X_4 - 0.00079X1^2 + 0.01271\, X_1X_2 - 0.0278X_1X_3 - 0.0021X_1X_4 + 0.176X_2X_3 + 1.6983X_2X_3 + 0.495X_3X_4 + \varepsilon$...........(2)

According to 95% confidence level, which means 0.05 probability (p) concept the model has been reduced. Table 8 shows the regression result table. From this analysis, the regression model after optimization differs more than the regression model after optimization for the MIG welding process parameter, which indirectly minimizes the amount of defect on the weld bead of medium carbon sheet metal steel. For this study, current is a more critical effect, and the combinations (interaction effect) of current, gas flow rate, current × voltage, current × travel speed, and voltage × gas flow rate are the significant effects, but factors and combinations have a negligible effect on the MIG welding process parameter.

$$dHV/d(1125 + 0.342X_1 - 29.41X_2 - 7.9X_3 - 62X_4 - 0.00079X1^2 + 0.01271\ X_1X_2 - 0.0278X_1X_3 - 0.0021X_1X_4 + 0.176X_2X_3 + 1.6983X_2X_4 + 0.495X_3X_4) + \varepsilon$$

The analysis has been done using coded units for the estimated regression coefficient for HV for MIG welding parameters. Simultaneously solve the four variables X_1, X_2, X_3 and X_4 are 150.14, 29.65V, 24.05mm/sec and13.85 lit/min respectively. So, the optimum value of the Hardness test is calculated as follows by substituting these optimum values of parameters in equation (2).

$$Hv = 1125 + 0.342(150.14) - 29.41(29.65) - 7.9(24.05) - 62(13.85) - 0.00079(150)^2 + 0.01271\ (150.14 \times 29.65) - 0.0278(150.14 \times 24.05) - 0.0021(150.14 \times 13.85) + 0.176(29.65 \times 24.05) + 1.6983(29.65 \times 13.85) + 0.495(24.05 \times 13.85 = \mathbf{178.29}$$

According to 95% confidence level, which means 0.05 probability (p) concept the model has been reduced. HV$Orgional$ = $170N/mm^2$MPa,$HV_{OPt=}$ = 178.29 N $/mm^2 for$ regression after optimization $\%HV_{improvement} = \frac{178.29-170}{170} \times 100\%$ = **4.876%,** regression after optimization.

From this analysis, the regression model after optimization is **4.876%** difference more than the regression model after optimization for the MIG welding process parameter, which indirectly minimizes the amount of enhancement on the weld bead of medium carbon sheet metal steel. For this study, the current gas flow rate is a more critical effect, and the combinations (interaction effect) of current with voltage, current with travel speed, and voltage with gas flow rate are significant effects, but factors and combinations have a negligible effect on the MIG welding process parameter [19].

3.4 Confirmation Experiment result

Table 9 above illustrates the final optimized settings and their corresponding outputs for identifying the optimal conditions to achieve the best welding product. To enhance the design settings for the welding operation experiment, it was conducted in two phases. Subsequently, this data was compared with the modified design of the experiment and then with the improved design of the experiment. The data collected from this experiment are presented in Table 9 which includes the confirmed settings for the design of the experiment, MT testing for the modified experiment, specimen drawing, and hardness testing of the specimens. The data compiled from this table indicates the HV output for both the improved and confirmed designs of the experiment.

Table 9 Improved Setting and its response hardness test

No	Current (Ampere)	Voltage (volte)	Travel speed (mm/s)	Gas flow rate (li/min)	Hardness test(HV result)
1	150.14	29.69	24.05	13.85	174
2	150.14	29.69	24.05	13.85	186
3	150.14	29.69	24.05	13.85	180
4	150.14	29.69	24.05	13.85	178
5	150.14	29.69	24.05	13.85	192
6	150.14	29.69	24.05	13.85	196

So from the mathematical analysis, the result has found that the percent improvement is hardness test **4.876%**% existed, modified and improved design of experiment, Source: (MINITAB software design package).

4. RESULT AND DISCUSSION

The detailed outcomes of the 22 experimental trials for both the existing and enhanced designs (refer to Tables 2 and 4) were examined utilizing Minitab and Design-Expert software, which validated that a quadratic model is statistically significant for the responses. This optimization endeavor sought to enhance the Vickers hardness (HV) while reducing enhancements in the medium-carbon steel plates measuring 100 mm×100 mm×6 mm, leading to post-weld hardness values that considerably surpassed the initial properties of the baseline material. Although the analytical ANOVA calculations indicated that travel speed is the most pivotal factor affecting weld quality, the RSM regression analysis emerged as the most objective and impartial approach for assessing factor contributions, ultimately achieving an optimized hardness test of 178.29 MPa—a 4.876% enhancement compared to the baseline model.

4.1 Hardness

Figure 7. The hardness profile across the HAZ of the 22 test pieces. From the figures, as we go through the section from the weld center, a higher hardness value reaching 188 HV is observed compared to HAZ, which has an average value of 159 HV, as well as the parent metal with an average value of 170 HV. From the experiments, in general, heat affect zone hardness is higher than the parent metal hardness by 18.5 %.

In some of the test pieces, one of the factors contributing to lower hardness in the HAZ zone is high heat input below its melting point, and hence retention of heat in this region. This phenomenon is observed in test pieces with small thickness and high input. The lower hardness in the HAZ might be explained by the intense grain growth in this region, resulting from high heat input below its melting point [19], [20].

The Vickers hardness pattern across the base metals and the welded seam is measured using a hardness tester. For the MIG-welded seam, the average hardness value ranges between 113 and 188 HV.

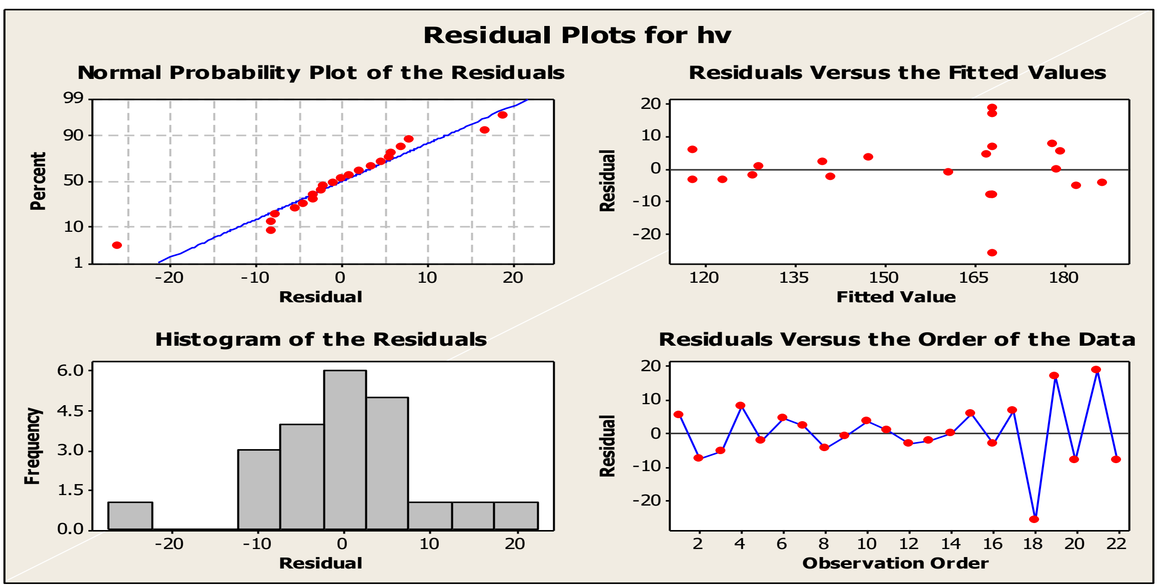

Figure 7: Residual graphs for existing DOE

From these residual graphs treated HV points are controlled with upper and lower limits. Whereas the following contour graphs and curvatures are plotted with lower response of HV values, which are directly related to I/P values.

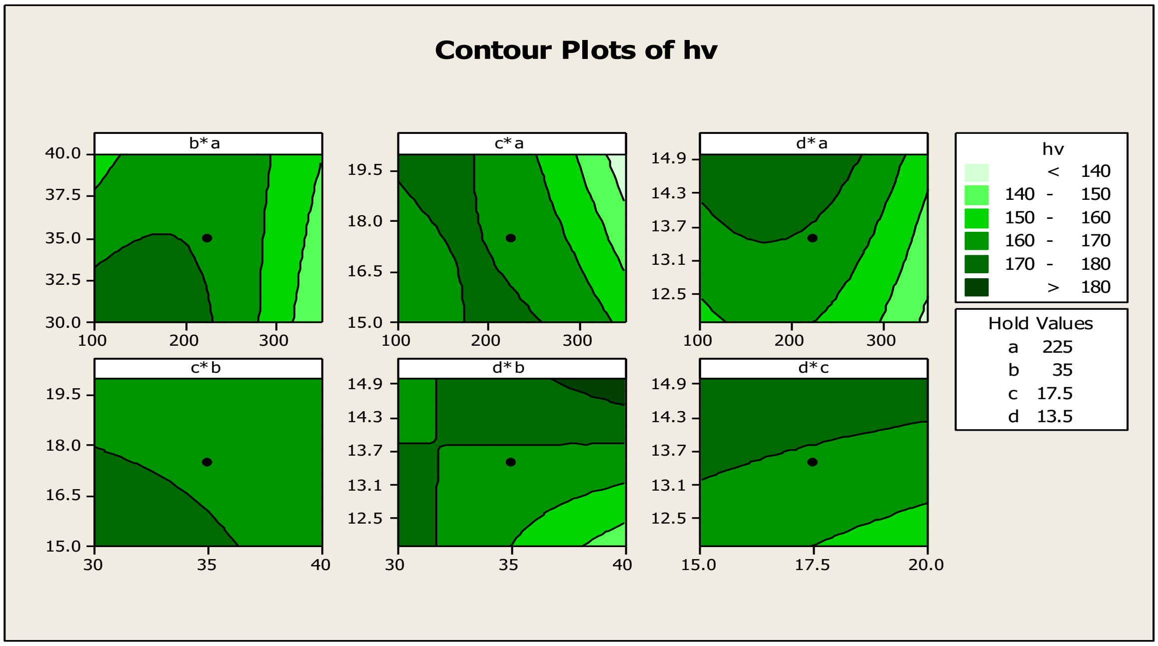

Figure 8 Contour graphs for existing DOE

Please refer to Figure 8. The contours of the response surface reveal that factor A exerts a predominant influence on Vickers hardness (HV), showcasing a notable quadratic effect. The vertical contour bands indicate that variations in factors c (ranging from 15 to 19.5) and d (spanning from 12.5 to 14.9) have minimal impact on HV. However, a slight interaction between factors b and a restricts the operational range for a x b to an approach of 40.

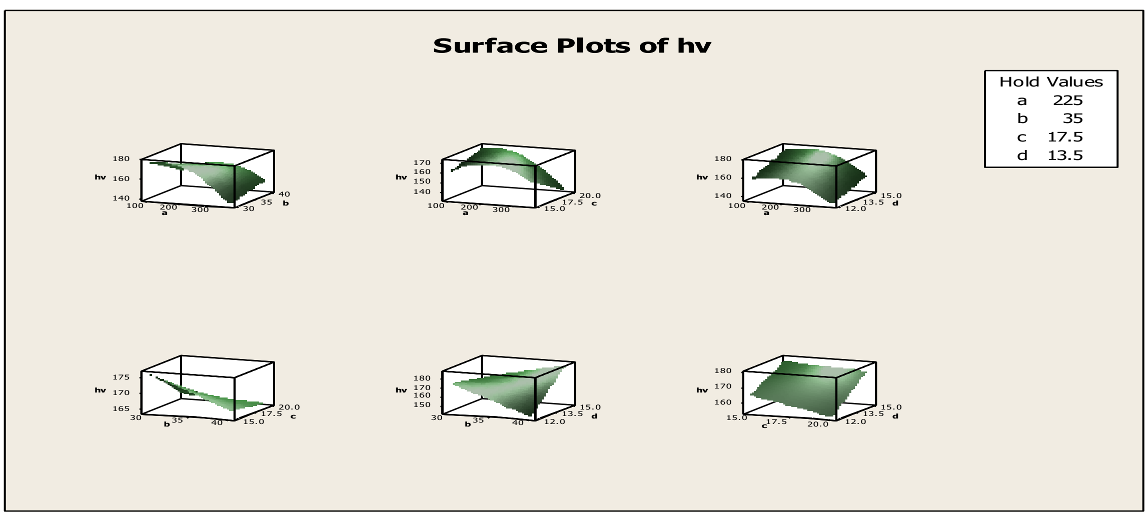

Figure 9 Surface graphs HV for Existing DOE

From these graphs, the combination of each parameter that affects the curvature of the graphs is different.

Figure 9 shows a surface plot of Hardness for the interaction of current and gas flow rate, when gap distances are taken as a hold value. This surface plot indicates that hardness increases with gas flow rate and current from 15 to 20 lit/min. and 100 to 350 Amps. But graph indicates that minor change have been seen on hardness by current. This surface plot indicates that hardness increase with decrease gas flow rate from 12 to 15 mm. as well as gas flow rate increase it will increase. It also shows that the `influence of both parameters is same.

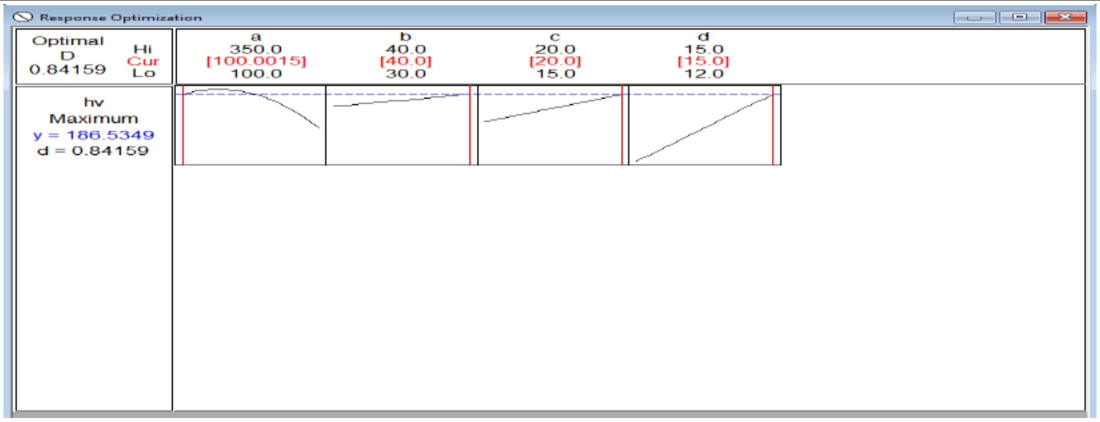

Figure 10 Optimal graphs HV for existed DOE

This provided optimal solutions for the input variable combinations, along with optimization plots shown in Fig 10 The optimization plot is interactive and input variable setting can be adjusted on the plot to search for more desirable solutions. Using the response optimizer, the maximum response (HV) for Current (A) = 150.14, Voltage (V) =29.65, travel Speed (mm/s) = 24.05, and gas flow rate (lit/min) = 13.85 has recommended. In order to verify the optimizer suggested values. The values of the input parameters from the response optimizer suggestion are first calculated and tests are conducted under the optimized conditions identified from RSM.

4.3 Verification Experiment and Optimal Graphs on the Improved Model

According to RSM techniques, to determine the optimal conditions and to compare the results with the expected conditions, it is necessary to perform a confirmation experiment. If the design fails to meet the specified requirement, the process must be reiterated using a new system until the required criteria are satisfied. The summary of the confirmation experiment data is given in Table 9 where the comparison between the starting and optimum condition are compared between predicted and achieved results [21].

4.4 Microstructure

The microstructure of a carbon steel plate welded by sub-automatic metal inert gas (MIG) welding has been evaluated, and the microstructure of each of the specimens at the weld, heat-affected zone, and parent metal is investigated. The results of the investigation indicate that significant grain coarsening was observed in the heat-affected zone (HAZ) of all the joints, and it was found that the extent of grain coarsening in the heat-affected zone increased with an increase in the heat input. The average dendrite length and inter-dendritic spacing in the weld zone were found to increase with the heat input [22].

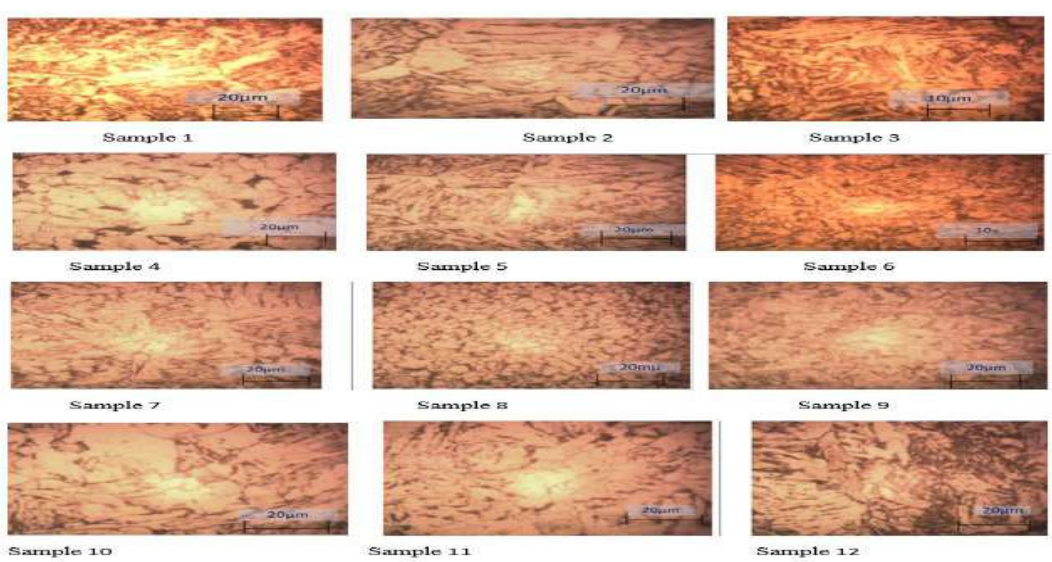

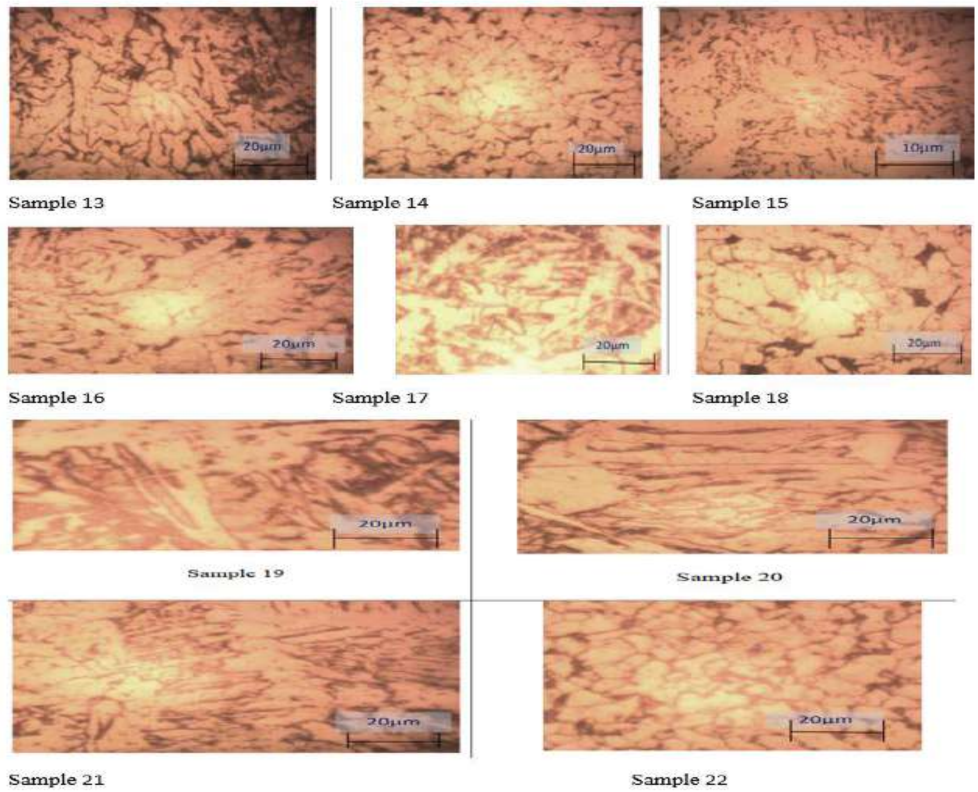

Figure 11 shows the microstructure of the weld zone at 200 A. As the current increase, the heat input also increases. The microstructure of the weld zone became more packed as the current increased from 200A to 230A. It can be observed that the microstructures at the weld zone are needle-like.

It was observed that increasing the welding current caused an increase in mechanical properties of welded metal. With increasing the input energy, grain size in the heat-affected zone of medium carbon steel AISI1035 showed a decrease in size of crystallite and the size of the grain boundaries increase. It will cause an increment in strength and hardness of welded metal. The phenomenon of grain growth does not occur as the grain size decrease and lead to recrystallization [23].

The microstructure of the medium carbon steel could not be seen clearly, perhaps due to under etching. A several samples of medium carbon steel were tried using the same etchant with different number of time but it still can't be seen clearly.

5.CONCLUSION AND RECOMMENDATION

5.1 Conclusions

Based on the experimental trials, Analysis of Variance (ANOVA), and RSM regression analysis, the following key conclusions are drawn: The ANOVA results demonstrate that a quadratic mathematical model provides the most accurate and reliable representation for predicting weld bead characteristics and joint performance. Welding current, welding voltage, travel speed, and gas flow rate are the most statistically significant parameters influencing the microstructure and resulting hardness profile of the MIG welded joint. proved to be a highly efficient, systematic, and cost-effective optimization tool. It successfully identified the optimal parameter combinations needed to achieve superior mechanical properties (such as balanced weld zone hardness) with a minimum number of experimental runs, significantly reducing manufacturing time and costs. The precise selection and control of these input parameters are critical factors in minimizing defects, preventing unwanted softening or embrittlement in the Heat-Affected Zone (HAZ), and achieving the optimal weld bead hardness and joint quality.

It is found that the parameter design of RSM provides a simple, systematic and efficient methodology for the optimization of the process parameters.

- The existed DOE design of parameter combination current setting is 150.14A, voltage 29.65, travel speed 24.05mm/sec and gas flow rate 13.85mm with optimum HV 178.29MPa.
- When the travel speed increasing the tensile strength also increasing, but all other parameters have reverse effect on HV.
- For modified DOE setting, the travel speed increases the hardness of the welded part increases from 170MPa to, 188MPa when the optimal values of the above parameters are experimentally increasing found to attain an optimal point.
- For improved (optimized) current as 100A, voltage 30 V, travel speed 15 mm/sec and gas flow rate 12mm with result of 186.5349MPa.
- According to regression analysis for RSM is 4.876% HV improvement.
- From the experiment with increase in heat in put there is an increase in width of Heat affected zone. When we compare the effect of welding speed and current on hardness, the effect of current is more significant than the effect due to travel speed
-

5.2 Recommendation

The following recommendations are made based on the study that has been conducted. It produces different types of metal products to fulfill the demand of customers. During the production using MIG welding process they face problems due to improper parameter combination for a specific material type. Hence, RSM parameter design is a best tool for reducing defects and to improve the HV weld bead. According to this study the following recommendations are advice to the factory**.**

- For welding 6 mm thick medium carbon steel plates, the optimized welding parameters identified in this study should be adopted to achieve improved weld bead hardness and overall weld quality.
- The recommended process parameters are a welding current of 100 A, arc voltage of 30 V, travel speed of 15 mm/s, and shielding gas flow rate of 12 L/min. These settings produced a weld bead hardness of approximately 186.53 MPa and can be used as a reference for production operations.
- Regular training and awareness programs should be provided for welders to enhance their understanding of parameter selection, welding techniques, and quality control practices.
- A standardized welding operation manual should be developed and implemented to ensure consistent application of process parameters, reduce welding defects, and improve product quality.
- The factory should periodically monitor and evaluate welding parameters to maintain process stability and ensure that the desired weld quality is consistently achieved.
- Future studies may investigate the effects of additional welding parameters, different material thicknesses, and alternative shielding gas compositions to further improve welding performance and productivity.

ACKNOWLEDGMENT

The author acknowledges the Manufacturing Industry Development Institute, Addis Ababa, Ethiopia, for providing the institutional support for this research. The contributions of the Manufacturing Technology & Engineering Industry Research Center and Akaki Basic Metal Industry that participated in the experimental data collection process are also gratefully acknowledged.

Declaration

The author declares no conflicts of interest regarding the publication of this manuscript.

Authors Biography

Shewangizaw Abu Abate received his M.Sc. degree in Mechanical Engineering Specialization Manufacturing Engineering from Bahir Dar University (Bahir Dar Institute of Technology). Currently, he serves as an Industrial Researcher at Manufacturing Industry Development Institute. His primary research interests lie in the fields of Additive manufacturing, welding, and Maintenance. His ongoing work focuses heavily on the optimization of manufacturing processes/industrial integration and strategic development within the sector. He has authored/papers in reputed journals and actively participates in industry-academic linkage initiatives.

REFERENCES

[1]. T. Kannan and N. Murugan,(2006) "Effect of flux cored arc welding process parameters on duplex stainless steel clad quality," J. Mater. Process. Technol., 176)1-3)230–239. doi: 10.1016/j.jmatprotec.2006.03.157.

[2]. M_A_Bodude,_I_Momohjimoh, "_Studies_on_Effects_of_Welding_Parameters (2).pdf," 2015.

[3]. T. N. Wordofa and P. J. Ramulu,(2023) "Gas Metal Arc Welding Input Parameters Impacts on Weld Quality Characteristics of Steel Materials a Comprehensive Exploration," Manuf. Technol., 23(3)3 366–379. doi: 10.21062/mft.2023.046.

[4]. A. Khorsheed et al.,(2025) "Process Optimization with Response Surface Methodology: A Comprehensive Approach by Experimental Design Types," Int. J. Adv. Nat. Sci. Eng. Res., 12(12)546–558, https://as-proceeding.com/index.php/ijanser

[5]. M. M. Ghogale and S. A. Patil,(2013) "Optimisation of process parameters of MIG welding to improve quality of weld by using Taguchi methodology.," Int. J. Eng. Res. Technol., 2(12) 3677–3685.

[6]. K. Y. Benyounis and A. G. Olabi,(2008) "Optimization of different welding processes using statistical and numerical approaches - A reference guide," Adv. Eng. Softw., 39(6)483–496. doi: 10.1016/j.advengsoft.2007.03.012.

[7]. D. Pang, W; Ahmed, N; and Dunne, "Hardness and microstructural gradients in the heat affected zone of welded low-carbon quenched and tempered steels.pdf," 2012.

[8]. M. Zaid Javed, E. Shara Khursheed, and M. Faizan Hasa,(2025) "Microstructure Analysis of Heat Affected Zone during MIG Welding Using Mild Steel," 13, 3.

[9]. S. B. P. Sanjay Kumar, Pravin K Singh, D Patel,(2017) "Optimization of Welding Parameters," 49(4)331–334.

[10]. American_Welding, "Welding_Handbook_Volume_2,_'Welding_Processes'_by_ (2).pdf."

[11]. P. K. Sivaraosa, K. R., Milkeya, Samsudina, A. K., "'Comparison between Taguchi method and response surface methodology (RSM) in modeling CO2 laser machining'.," 2014.

[12]. B. . Phafat, N.G., and Shukla, "'Experimental study of CO2 arc welding parameters on weld strength for AISI 1022 steel plates using response surface methodology'.," 2013.

[13]. T. F. d. A. Souto, J. I. V. d., Ferreira, S. D., Lima, J. S. d., Castro, W. B. d., Grassi, E. N. D., & Santos, "The impact of GMAW process parameters and heat input on the weld overlay of austenitic stainless steel 316L-Si.," 2023.

[14]. J. Xia, S. Liu, B. ZHang, and Y. Chen, "Central Composite Experiment Design (CCD) -Response," no. Ccd, 2021.

[15]. Berrin_Ozkaya_and_Yasemin_Genc Mustafa_AgahTekindal, _Hülya_Bayrak, "'Box-Behnken experimental design in factorial experiments: the importance of bread for nutrition and health'.," 2012.

[16]. A. Ardian, C. Gunawan, P. Hargiyarto, and K. Syauqi, (2023)"Magnetic particle testing on student welding practice results based on AWS and ASME standards," AIP Conf. Proc., 2671, doi: 10.1063/5.0119984.

[17]. T. Kurşun, "The influence of GMAW and GMAW-P welding processes on the microstructure, hardness, tensile, and impact strength of AISI 1030 steel joints created with ASP316L austenitic stainless steel filler.pdf," 2011.

[18]. O. O. F. Fca,(2025) "Welding is a vital industrial process for joining metals and thermoplastics , with Metal InertGas (MIG) and Flux Cored Arc (FCA) welding widely used due to their versatility and effectiveness . This study optimized FCA and MIG welding parameters for ," 44(4)1–14.

[19]._Pratibha_K Mohd_S, _Mohd_P, ""Effect_of_MIG_welding_input_process (2).pdf," 2013.

[20]. V. Thangavel, S. Maheswari, C., Priyanka, E. B., Stonier, A. A., Peter, G., & Ganji, "An analysis and optimization of the automated TIG

welding process parameters on SS304 utilizing the Taguchi optimization.pdf," 2024.

[21]. C. M. Stevens, N. T., & Anderson-Cook, "Design and analysis of confirmation experiments. Journal of Quality Technology," 2019.

[22]. S. Kumar and A. S. Shahi,(2011) "Effect of heat input on the microstructure and mechanical properties of gas tungsten arc welded AISI 304 stainless steel joints," Mater. Des., 32(6)3617–3623, doi: 10.1016/j.matdes.2011.02.017.

[23]. y C. N. Christopher, N. Mbah1, Bonaventure, C. Ugwuanyi, Kingsle,(2019) "Effect of Welding Parameters on the Mechanical Properties of Friction-Stir-Welded Heat-Treatable Aa6061-T6," Vietnam J. Sci. Technol., 57(6) 677–684. doi: 10.15625/2525-2518/57/6/13808.